

alpha-nucleus potentials for the neutron-deficient p nuclei

P. Mohr

Institut für Kernphysik, Technische Universität Darmstadt, Schlossgartenstrasse 9, D-64289 Darmstadt, Germany
(March 14, 2021)

α -nucleus potentials are one important ingredient for the understanding of the nucleosynthesis of heavy neutron-deficient p nuclei in the astrophysical γ -process where these p nuclei are produced by a series of (γ, n) , (γ, p) , and (γ, α) reactions. I present an improved α -nucleus potential at the astrophysically relevant sub-Coulomb energies which is derived from the analysis of α decay data and from a previously established systematic behavior of double-folding potentials.

PACS numbers: 23.60.+e, 25.55.Ci, 26.30.+k, 26.45.+h

I. INTRODUCTION

The bulk of the heavy nuclei ($A \geq 100$) has been synthesized by neutron capture in the s - and r -process. However, most of the rare neutron-deficient nuclei with $A \geq 100$ cannot be produced by neutron capture. The main production mechanism for these so-called p nuclei is photodisintegration in the astrophysical γ -process by (γ, n) , (γ, p) , and (γ, α) reactions of heavy seed nuclei from the s - and r -process. A list of the neutron-deficient p nuclei from ^{74}Se to ^{196}Hg can be found in Table 1 of Ref. [1]. Typical parameters for the γ -process are temperatures of $2 \leq T_9 \leq 3$ (T_9 is the temperature in GK), densities of about 10^6 g/cm^3 , and time scales in the order of one second. Several astrophysical sites for the γ -process have been proposed, and the oxygen- and neon-rich layers of type II supernovae seem to be a good candidate. However, there has been no definite conclusion reached yet with respect to the astrophysical site where the γ -process occurs. Details about the astrophysical scenarios can be found in the reviews by Lambert [1], Arnould and Takahashi [2], Wallerstein *et al.* [3], and in Refs. [4–8].

Almost no experimental data exist for the cross sections of the γ -induced reactions at astrophysically relevant energies. Therefore, all reaction rates have been derived theoretically using statistical model calculations. One striking example is ^{146}Sm which is a potential chronometer for the γ -process. The production ratio of ^{146}Sm and ^{144}Sm depends sensitively on the (γ, n) and (γ, α) cross sections at the branching nucleus ^{148}Gd , and it has been shown that especially the (γ, α) cross section can be calculated only if a reliable α -nucleus potential is available. Predictions from different potentials differ by one order of magnitude [9–12]. The need for improved α -nucleus potentials for astrophysical calculations has been pointed out in [13,14].

Systematic α -nucleus potentials have been presented in several papers (e.g. Refs. [15–17]), and recently these studies have been extended to astrophysically relevant energies [13,14]. Usually potentials are derived from scattering data. However, at the astrophysically relevant energies below the Coulomb barrier it is difficult to derive the potential from the experimental data unambiguously (see e.g. [11]). Alternatively, the cluster model provides another possibility to determine α -nucleus potentials by an adjustment of the α -nucleus potential to the bound state properties of the nucleus $(A + 4) = A \otimes \alpha$ [18–20]. The half-lives of many α emitters have been calculated in [21,22] using a specially shaped potential, but this potential had to be modified to describe elastic scattering for ^{208}Pb [23]. It has been shown in Refs. [24,17] that a systematic double-folding potential is able to reproduce both the bound state properties of $^{212}\text{Po} = ^{208}\text{Pb} \otimes \alpha$ and elastic α scattering of ^{208}Pb . Finally, folding potentials give an excellent description of the experimental data on ^{144}Sm at 20 MeV [11], but again the potential which was used for the calculation of the α decay data [21] is not able to reproduce the precision scattering data.

The basic idea of this work is to determine the α -nucleus potential at astrophysically relevant energies of about 5 to 12 MeV which is in the energy gap between the bound state potentials and the scattering potentials. I have chosen double folding potentials because of the small numbers of adjustable parameters. A systematic behavior of the strength of double folding potentials at higher energies is already given in Ref. [17]. In this work I will analyze bound state properties. First, I will briefly present the method in Sect. II, then I will give results for the neutron-deficient α emitting p nuclei in Sect. III, and finally I will give an outlook on possible further improvements of the α -nucleus potentials (Sect. IV).

II. FOLDING POTENTIALS AND α DECAY

The α decay of nuclei is a clear proof that the wave function of the α emitting nucleus $A + 4$ has a non-negligible component $A \otimes \alpha$, whereas low-energy elastic scattering is described using a pure $A \otimes \alpha$ wave function. Therefore, an effective α -nucleus potential should describe simultaneously the half-life of the α emitter $A + 4$ and elastic α scattering of the nucleus A . In the astrophysically relevant energy region the α -nucleus potential is accessible mainly from the decay data because elastic scattering is dominated by the Coulomb interaction. For the analysis of the α decay data I apply the semi-classical model of Ref. [25], and the nuclear potentials $V_N(r)$ are calculated by the double-folding procedure:

$$V_N(r) = \lambda V_F(r) = \lambda \int \int \rho_P(r_P) \rho_T(r_T) v_{\text{eff}}(E, \rho = \rho_P + \rho_T, s = |\vec{r} + \vec{r}_P - \vec{r}_T|) d^3 r_P d^3 r_T \quad (2.1)$$

where ρ_P, ρ_T are the densities of projectile resp. target, and v_{eff} is the effective nucleon-nucleon interaction taken in the well-established DDM3Y parametrization [26,27]. Details about the folding procedure can be found in Refs. [19,17], the folding integral (2.1) has been calculated using the code DFOLD [28]. The strength of the folding potential is adjusted by the usual strength parameter λ with $\lambda \approx 1.1 - 1.3$ leading to volume integrals J_R per interacting nucleon pair of about 300 to 350 MeV fm³. J_R is defined by

$$J_R = \frac{4\pi}{A_P A_T} \int_0^\infty V_N(r) r^2 dr \quad . \quad (2.2)$$

Note that in the discussion of volume integrals J usually the negative sign is neglected; also in this paper all J values are negative.

The densities of the nuclei have been derived from the experimentally known charge density distributions [29] and assuming identical proton and neutron distributions. For nuclei where no experimental charge density distribution is available (i) the density distribution of the closest neighboring isotope was used with an adjusted radius parameter $R \sim A^{1/3}$ (¹⁸⁶Os, ¹⁸²W, ¹⁷⁰Yb, ¹⁵⁰Gd), (ii) the average between two neighboring stable isotopes was used (¹⁴⁶Sm) and (iii) the average of ¹³⁸Ba and ¹⁴²Nd was used for ¹⁴⁰Ce.

The total potential is given by the sum of the nuclear potential $V_N(r)$ and the Coulomb potential $V_C(r)$:

$$V(r) = V_N(r) + V_C(r) \quad . \quad (2.3)$$

The Coulomb potential is taken in the usual form of a homogeneously charged sphere where the Coulomb radius R_C has been chosen identically with the *rms* radius of the folding potential V_F .

The potential strength parameter λ was adjusted to the energy of the α particle in the α emitter $(A + 4) = A \otimes \alpha$. The number of nodes of the bound state wave function was taken from the Wildermuth condition

$$Q = 2N + L = \sum_{i=1}^4 (2n_i + l_i) = \sum_{i=1}^4 q_i \quad (2.4)$$

where Q is the number of oscillator quanta, N is the number of nodes and L the relative angular momentum of the α -core wave function, and $q_i = 2n_i + l_i$ are the corresponding quantum numbers of the nucleons in the α cluster. I have taken $q = 4$ for $50 < Z, N \leq 82$, $q = 5$ for $82 < Z, N \leq 126$, and $q = 6$ for $N > 126$ where Z and N are the proton and neutron number of the daughter nucleus (see also Table I).

The α decay width Γ_α is given by the following formulae [25]:

$$\Gamma_\alpha = PF \frac{\hbar^2}{4\mu} \exp \left[-2 \int_{r_2}^{r_3} k(r) dr \right] \quad (2.5)$$

with the preformation factor P , the normalization factor F

$$F \int_{r_1}^{r_2} \frac{dr}{k(r)} = 1 \quad (2.6)$$

and the wave number $k(r)$

$$k(r) = \sqrt{\frac{2\mu}{\hbar^2} |E - V(r)|} \quad . \quad (2.7)$$

μ is the reduced mass and E is the decay energy of the α decay which was taken from the computer files based on the mass table of Ref. [30]. The r_i are the classical turning points. For $0^+ \rightarrow 0^+$ s -wave decay the inner turning point is at $r_1 = 0$. r_2 varies from about 7 to 9 fm, and r_3 varies from 45 up to about 90 fm. The decay width Γ_α is related to the half-life by the well-known relation $\Gamma_\alpha = \hbar \ln 2 / T_{1/2}$.

It has to be pointed out that the preformation factor P should be smaller than unity because the simple two-body model assumes that the ground state wave function of the α emitter $A + 4$ contains a pure $A \otimes \alpha$ configuration. The decay width in this model therefore always overestimates the experimental decay width. I determine the preformation factor P from the ratio between the calculated and the experimental half-lives [31]. A strong $A \otimes \alpha$ cluster component is expected for nuclei A with magic proton and/or neutron numbers, and indeed the calculations show increased values for P around $N = 126$ (^{208}Pb) and $N = 82$ (e.g. ^{140}Ce) (see Table I).

A preformation factor of $P = 1$ as used in [21] seems to be the consequence of the specially shaped cosh potential of that work. As an example I compare the potentials $V(r) = V_N(r) + V_C(r)$ from this work and from [21] for the system $^{190}\text{Pt} = ^{186}\text{Os} \otimes \alpha$ in Fig. 1. The *rms* radius of the potential from [21] is significantly smaller ($r_{rms} = 5.58$ fm) than the *rms* radius of the folding potential ($r_{rms} = 5.97$ fm). Therefore, the Coulomb barrier in [21] is significantly higher and the calculated half-lives in [21] are roughly one order of magnitude larger than in this work. Note that in [21] the potential was adjusted only to decay properties with the assumption $P = 1$ whereas in this work an effective potential is presented which is designed to describe decay properties and scattering wave functions and which leads to realistic preformation factors P .

III. RESULTS FOR NEUTRON-DEFICIENT α EMITTERS

The results of the calculations are summarized in Table I and shown in Fig. 2. One important result is that the strength parameters λ and the volume integrals J_R for all α emitters show only small variations over the analyzed mass region $A \geq 140$. This means that the α -nucleus potential is well defined at very low energies. As expected from the systematic study in [17], for the light system $^8\text{Be} = ^4\text{He} \otimes \alpha$ a much higher volume integral is required.

The preformation factors P systematically increase to smaller masses with local maxima around the magic neutron numbers $N = 82$ and $N = 126$. The very high value of $P = 65\%$ for ^8Be is not surprising because of the well-known α cluster structure of this nucleus.

One further exception is found for $^{174}\text{Hf} = ^{170}\text{Yb} \otimes \alpha$ with $P = 62.8\%$. However, this surprisingly large value reduces to $P = 3.13\%$ if the energy $E = 2.584$ MeV from [21] is taken which was derived from the measured α energy and corrected for recoil and atomic effects instead of $E = 2.4948$ MeV from [30]. On the other hand, the uncertainty of the measured half-life of ^{174}Hf is also 20%, and a previous experiment gives a half-life which is roughly a factor of 2 higher [31]. From these calculations I have strong evidence that there is an inconsistency in the system $^{174}\text{Hf} = ^{170}\text{Yb} \otimes \alpha$ between the measured half-life, the α energy, and the masses from the mass table [30].

IV. CONCLUSIONS AND OUTLOOK

The real part of the optical potential is well defined by the systematic study of scattering data at higher energies above about 20 MeV and by the adjustment of the potential to the bound state properties at very low energies (see Fig. 3). An interpolation between these energy regions leads to the recommended volume integral which is shown in Fig. 3 as full line. A Gaussian parametrization is applied to J_R :

$$J_R(E) = J_{R,0} \times \exp[-(E - E_0)^2 / \Delta^2] \quad (4.1)$$

with $J_{R,0} = 350$ MeV fm³, $E_0 = 30$ MeV, and $\Delta = 75$ MeV. This interpolation is valid from very low energies up to about 40 MeV.

The energy dependence of J_R at low energies is $\Delta J_R / \Delta E \approx 1.7$ MeV fm³ / MeV, in agreement with $\Delta J_R / \Delta E = 1 - 2$ MeV fm³ / MeV [11] and somewhat larger than $\Delta J_R / \Delta E = 0.71$ MeV fm³ / MeV [14]. The uncertainty of an interpolated value of J_R is significantly smaller than 10 MeV fm³ corresponding to about 3% in the interesting energy range around 10 MeV.

Whereas the real part of the potential is well defined, no experimental information is available for the imaginary part of the potential at very low energies. However, it has been shown that transmission coefficients and cross sections in statistical model calculations depend sensitively on the volume integral J_I and even the shape of the imaginary part of the potential. Fig. 3 shows also the volume integrals J_I of the imaginary part of the potential for the same nuclei together with a parametrization from [32]. A different parametrization of the energy dependence of J_I has been presented in [14]. Because of the very similar behavior of ^{90}Zr and ^{144}Sm further information could be obtained

from α scattering in the $A \approx 100$ region where the energy region between 10 and 20 MeV might be accessible for high-precision scattering experiments. Note that in the ^{144}Sm case an analysis of scattering data below $E = 20$ MeV [11] is very difficult because of the dominating Coulomb interaction.

New experiments in the $A \approx 100$ region are planned. If carried out with sufficient precision, the predictions of this work for the real part of the potential can be tested and new information on the imaginary part can be derived.

ACKNOWLEDGMENTS

Discussions with H. Oberhummer, E. Somorjai, G. Staudt, and A. Zilges are gratefully acknowledged.

- [1] D. L. Lambert, *Astron. Astrophys. Rev.* **3**, 201 (1992).
- [2] M. Arnould and K. Takahashi, *Rep. Prog. Phys.* **62**, 395 (1999).
- [3] G. Wallerstein *et al.*, *Rev. Mod. Phys.* **69**, 995 (1997).
- [4] K. Ito, *Prog. Theor. Phys.* **26**, 990 (1961).
- [5] S. E. Woosley and W. M. Howard, *Astrophys. J. Suppl.* **36**, 285 (1978).
- [6] M. Rayet, N. Prantzos, and M. Arnould, *Astron. Astrophys.* **227**, 271 (1990).
- [7] N. Prantzos, M. Hashimoto, M. Rayet, and M. Arnould, *Astron. Astrophys.* **238**, 455 (1990).
- [8] W. M. Howard, B. S. Meyer, and S. E. Woosley, *Astrophys. J.* **373**, L5 (1991).
- [9] S. E. Woosley and W. M. Howard, *Astrophys. J.* **354**, L21 (1990).
- [10] T. Rauscher, F.-K. Thielemann, and H. Oberhummer, *Astrophys. J.* **451**, L37 (1995).
- [11] P. Mohr, T. Rauscher, H. Oberhummer, Z. Máté, Zs. Fülöp, E. Somorjai, M. Jaeger, and G. Staudt, *Phys. Rev. C* **55**, 1523 (1997).
- [12] E. Somorjai, Zs. Fülöp, Á. Z. Kiss, C. Rolfs, H. P. Trautvetter, U. Greife, M. Junker, S. Goriely, M. Arnould, M. Rayet, T. Rauscher, and H. Oberhummer, *Astron. Astrophys.* **333**, 1112 (1998).
- [13] T. Rauscher, *Proc. Nuclei in the Cosmos V*, Volos, Greece, 06.-11. July 1998, Ed. N. Prantzos and S. Harissopulos, Editions Frontières, Paris, 1998.
- [14] C. Grama and S. Goriely, *Proc. Nuclei in the Cosmos V*, Volos, Greece, 06.-11. July 1998, Ed. N. Prantzos and S. Harissopulos, Editions Frontières, Paris, 1998.
- [15] F. M. Mann, *Hanford Engineering HEDL-TME*, p. 78 (1978).
- [16] V. Avrigeanu, P. E. Hodgson, and M. Avrigeanu, *Phys. Rev. C* **49**, 2136 (1994).
- [17] U. Atzrott, P. Mohr, H. Abele, C. Hillenmayer, and G. Staudt, *Phys. Rev. C* **53**, 1336 (1996).
- [18] F. Michel and R. Wanderpoorten, *Phys. Rev. C* **16**, 142 (1977).
- [19] H. Abele and G. Staudt, *Phys. Rev. C* **47**, 742 (1993).
- [20] B. Buck, A. C. Merchant, and S. M. Perez, *Phys. Rev. C* **51**, 559 (1995).
- [21] B. Buck, A. C. Merchant, and S. M. Perez, *At. Data Nucl. Data Tab.* **54**, 53 (1993).
- [22] B. Buck, A. C. Merchant, and S. M. Perez, *Phys. Rev. C* **54**, 2063 (1996).
- [23] B. Buck, J. C. Johnston, A. C. Merchant, and S. M. Perez, *Phys. Rev. C* **53**, 2841 (1996).
- [24] F. Hoyler, P. Mohr, and G. Staudt, *Phys. Rev. C* **50**, 2631 (1994).
- [25] S. A. Gurvitz and G. Kälbermann, *Phys. Rev. Lett.* **59**, 262 (1987).
- [26] G. R. Satchler and W. G. Love, *Phys. Rep.* **55**, 183 (1979).
- [27] A. M. Kobos, B. A. Brown, R. Lindsay, and R. Satchler, *Nucl. Phys.* **A425**, 205 (1984).
- [28] H. Abele, Univ. Tübingen, computer code DFOLD, unpublished.
- [29] H. de Vries, C. W. de Jager, and C. de Vries, *Atomic Data and Nuclear Data Tables* **36**, 495 (1987).
- [30] G. Audi and A. H. Wapstra, *Nucl. Phys.* **A595**, 409 (1995).
- [31] ENSDF data base, revision of 3-Dec-1999, using NNDC Online Data Service.
- [32] G. E. Brown and M. Rho, *Nucl. Phys.* **A372**, 397 (1981).

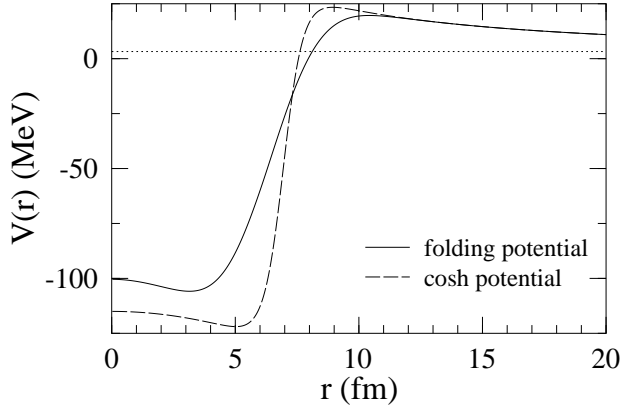


FIG. 1. Comparison of the potentials $V(r) = V_N(r) + V_C(r)$ from this work (folding potential, full line) and from [21] (specially shaped cosh potential, dashed line) for the system $^{190}\text{Pt} = ^{186}\text{Os} \otimes \alpha$. The decay energy E is indicated by a dotted line. Note the significantly higher Coulomb barrier in [21] compared to the folding potential.

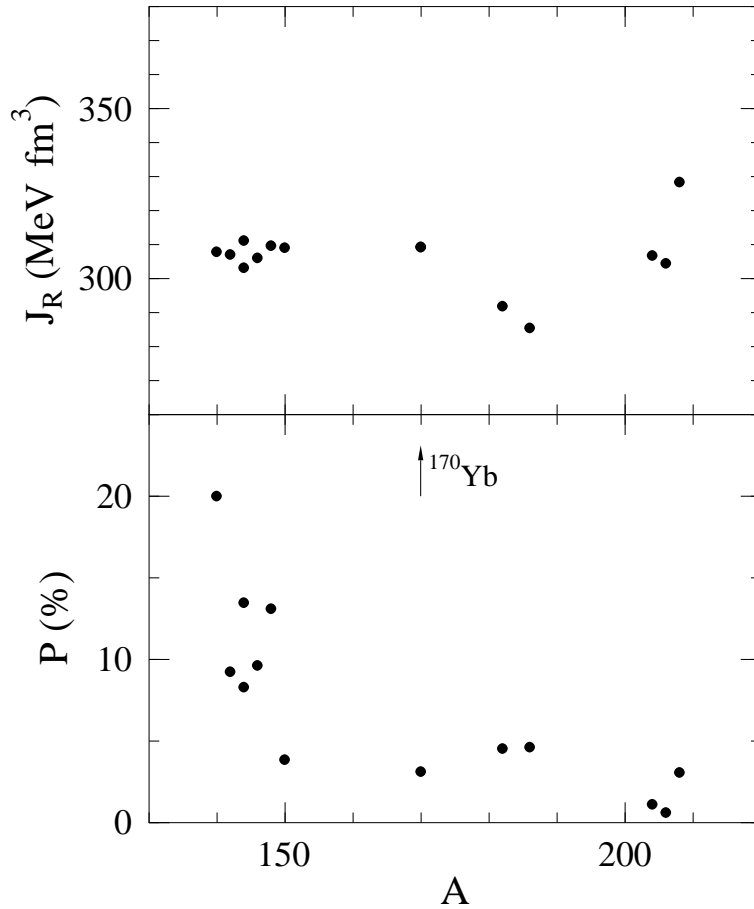


FIG. 2. The volume integrals J_R (upper diagram) and the preformation factors P (lower diagram) are shown for several neutron-deficient α emitters. The variation of the volume integrals J_R with A is small, whereas the preformation factor P increases to lower mass numbers A . Local maxima for P can be found around $A = 144$ and $A = 208$ corresponding to the magic neutron numbers $N = 82$ and $N = 126$. For $^{174}\text{Hf} = ^{170}\text{Yb} \otimes \alpha$ the value derived from $E = 2.584$ MeV [21] is shown; the value derived from $E = 2.4948$ MeV [30] exceeds the scale of the diagram and is indicated by an arrow (see text and Table I).

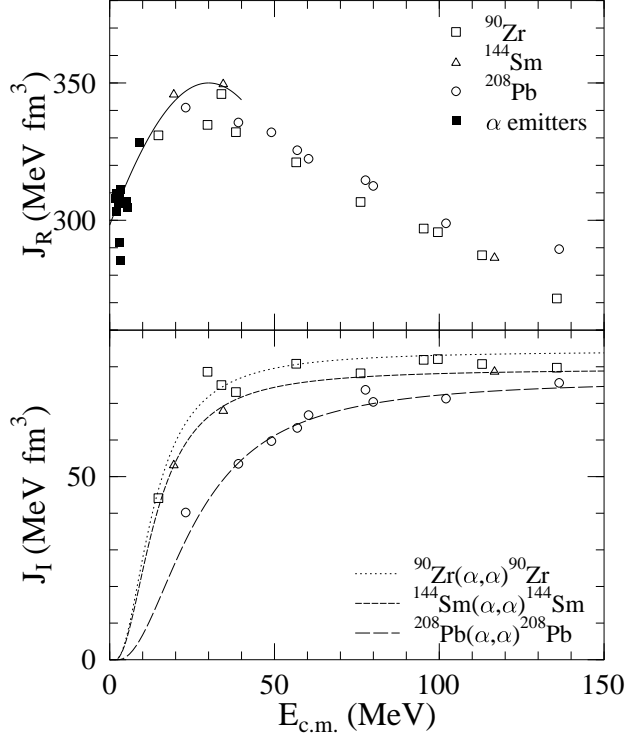


FIG. 3. Volume integrals J_R (upper diagram) derived from α decay data (this work) and from elastic scattering [17,11] for the nuclei ^{90}Zr , ^{144}Sm , and ^{208}Pb . The full line shows the recommended interpolation for the astrophysically relevant energy region. The lower diagram shows the volume integral J_I of the imaginary part of the potential for the same nuclei together with Brown-Rho parametrizations [32] (dashed and dotted lines). This figure is combined from data of [17,11].

TABLE I. Experimental and theoretical decay widths of several neutron-deficient α emitters (parent). The light α emitter ^8Be has been added.

parent	daughter	E (MeV)	Q	λ	J_R (MeV fm ³)	$T_{1/2}^{\text{calc}}$ (y)	$T_{1/2}^{\text{exp}}$ (y)	P (%)
^{212}Po	^{208}Pb	8.9541	22	1.241	328.4	9.20×10^{-9} s	$(2.99 \pm 0.02) \times 10^{-7}$ s	3.08 ^a
^{210}Po	^{206}Pb	5.4075	20	1.148	304.5	2.35×10^{-3}	0.37886 ± 0.00001	0.62
^{208}Po	^{204}Pb	5215.5	20	1.157	306.8	3.27×10^{-2}	2.898 ± 0.002	1.13
^{190}Pt	^{186}Os	3.2495	18	1.067	285.5	3.01×10^{10}	$(6.5 \pm 0.3) \times 10^{11}$	4.63
^{186}Os	^{182}W	2.8220	18	1.078	291.9	9.08×10^{13}	$(2.0 \pm 1.1) \times 10^{15}$	4.54
^{174}Hf	^{170}Yb	2.4948	18	1.116	309.3	1.26×10^{15}	$(2.0 \pm 0.4) \times 10^{15}$	62.8 ^b
^{154}Dy	^{150}Gd	2.9466	18	1.125	309.1	1.16×10^5	$(3.0 \pm 1.5) \times 10^6$	3.86
^{152}Gd	^{148}Sm	2.2046	18	1.146	309.7	1.42×10^{13}	$(1.08 \pm 0.08) \times 10^{14}$	13.1
^{150}Gd	^{146}Sm	2.8089	18	1.141	306.1	1.73×10^5	$(1.79 \pm 0.08) \times 10^6$	9.65
^{148}Gd	^{144}Sm	3.2712	18	1.159	311.2	6.20	74.6 ± 3.0	8.31
^{148}Sm	^{144}Nd	1.9860	18	1.123	303.2	1.08×10^{15}	$(8 \pm 2) \times 10^{15}$	13.5
^{146}Sm	^{142}Nd	2.5289	18	1.138	307.1	9.53×10^6	$(1.03 \pm 0.05) \times 10^8$	9.25
^{144}Nd	^{140}Ce	1.9052	18	1.147	307.9	4.58×10^{14}	$(2.29 \pm 0.16) \times 10^{15}$	20.0
^8Be	^4He	0.0919	4	1.624	444.2	4.34×10^{-17} s	$(6.71 \pm 1.68) \times 10^{-17}$ s	64.6

^a Minor differences between the preformation factor P in Ref. [24] and this work are due to the different choice of the Coulomb radius: $R_C = 1.2 \text{ fm} \times A_T^{1/3} = 7.11 \text{ fm}$ [24] and $R_C = 6.099 \text{ fm} = r_{rms}$ (this work).

^b A value of $P = 3.13\%$ is achieved with the energy $E = 2.584 \text{ MeV}$ from Ref. [21] (see text).